Clinical Cancer Research

The ETS Inhibitors YK-4-279 and TK-216 Are Novel Antilymphoma Agents

Filippo Spriano[1], Elaine Yee Lin Chung[1], Eugenio Gaudio[1], Chiara Tarantelli[1], Luciano Cascione[1,2], Sara Napoli[1], Katti Jessen[3], Laura Carrassa[4], Valdemar Priebe[1], Giulio Sartori[1], Garrett Graham[5], Saravana P. Selvanathan[5], Andrea Cavalli[6], Andrea Rinaldi[1], Ivo Kwee[1,2,7], Monica Testoni[1], Davide Genini[1], B. Hilda Ye[8], Emanuele Zucca[9], Anastasios Stathis[9], Brian Lannutti[3], Jeffrey A. Toretsky[5], and Francesco Bertoni[1]

Abstract

Purpose: Transcription factors are commonly deregulated in cancer, and they have been widely considered as difficult to target due to their nonenzymatic mechanism of action. Altered expression levels of members of the ETS-transcription factors are often observed in many different tumors, including lymphomas. Here, we characterized two small molecules, YK-4-279 and its clinical derivative, TK-216, targeting ETS factors via blocking the protein–protein interaction with RNA helicases, for their antilymphoma activity.

Experimental Design: The study included preclinical *in vitro* activity screening on a large panel of cell lines, both as single agent and in combination; validation experiments on *in vivo* models; and transcriptome and coimmunoprecipitation experiments.

Results: YK-4-279 and TK-216 demonstrated an antitumor activity across several lymphoma cell lines, which we validated *in vivo*. We observed synergistic activity when YK-4-279 and TK-216 were combined with the BCL2 inhibitor venetoclax and with the immunomodulatory drug lenalidomide. YK-4-279 and TK-216 interfere with protein interactions of ETS family members SPIB, in activated B-cell–like type diffuse large B-cell lymphomas, and SPI1, in germinal center B-cell–type diffuse large B-cell lymphomas.

Conclusions: The ETS inhibitor YK-4-279 and its clinical derivative TK-216 represent a new class of agents with *in vitro* and *in vivo* antitumor activity in lymphomas. Although their detailed mechanism of action needs to be fully defined, in DLBCL they might act by targeting subtype-specific essential transcription factors.

Introduction

The erythroblastosis virus E26 transformation specific (ETS)-transcription factors family comprises 28 proteins sharing a conserved DNA-binding domain (1). Altered ETS gene expression levels are often observed in many different tumors, including lymphomas (2–6). ETS1 and FLI1 are recurrently gained in approximately 25% of the cases of diffuse large B-cell lymphoma (DLBCL; ref. 3). *SPIB* is overexpressed as a consequence of translocation of the *IgH* locus to chromosome 19 (4) or recurrent DNA gains in about 25% of activated B-cell–like (ABC) DLBCL (5). Silencing experiments have shown that SPIB is indeed an essential gene for the ABC-DLBCL, while *SPI1* is necessary for the survival of germinal center B-cell–type (GCB) DLBCL (5–7).

Transcription factors have been widely considered difficult to target due to their nonenzymatic mechanism of action. They often complex with RNA helicases; these enzymes have emerged as key regulators of cellular transformation in cancer (8). One example is RNA helicase A (DHX9 or RHA), an enzyme with many functions including translation and splicing. EWS-FLI1 is an Ewing sarcoma (ES) specific fusion oncogene that requires DHX9 for neoplastic transformation (9, 10). YK-4-279 is a small molecule that binds to EWS-FLI1 and blocks its interaction with DHX9, resulting in growth arrest and apoptosis in ES cells (9). This disruption of protein interaction rather than inhibition of a relatively ubiquitous enzyme is believed to provide relative specificity for cancer cells. YK-4-279 can also affect other ETS transcription factors, such as ERG and ETV1 in prostate cancer cells (11–14). TK-216 is a derivative developed for clinical trials with demonstrated *in vitro* and *in vivo* antitumor activity in ES models (15). TK-216 is a first-in-class inhibitor of the ETS family that is currently in phase I trials for patients with relapsed/refractory ES (NCT02657005; ref. 16). Although the mechanism of action of YK-4-279 and TK-216 has

[1]Università della Svizzera italiana, Institute of Oncology Research, Bellinzona, Switzerland. [2]Swiss Institute of Bioinformatics, Lausanne, Switzerland. [3]Oncternal Therapeutics, San Diego, California. [4]Department of Oncology, IRCCS-Istituto di Ricerche Farmacologiche Mario Negri, Milan, Italy. [5]Departments of Oncology and Pediatrics, Lombardi Comprehensive Cancer Center, Georgetown University, Washington, DC. [6]Università della Svizzera italiana, Institute of Biomedical Research, Bellinzona, Switzerland. [7]Dalle Molle Institute for Artificial Intelligence, Manno, Switzerland. [8]Department of Cell Biology, Albert Einstein College of Medicine and Montefiore Medical Center, Bronx, New York, New York. [9]Oncology Institute of Southern Switzerland, Bellinzona, Switzerland.

Note: Supplementary data for this article are available at Clinical Cancer Research Online (http://clincancerres.aacrjournals.org/).

F. Spriano and E.Y.L. Chung contributed equally to this article.

Corresponding Author: Francesco Bertoni, Università della Svizzera italiana, via Vela 6, Bellinzona 6500, Switzerland. Phone: 41-91-820-0367; Fax: 41-91-820-0397; E-mail: frbertoni@mac.com

Clin Cancer Res 2019;25:5167–76

doi: 10.1158/1078-0432.CCR-18-2718

©2019 American Association for Cancer Research.

Downloaded from http://aacrjournals.org/clincancerres/article-pdf/25/16/5167/1933678/5167.pdf by guest on 25 January 2025

Translational Relevance

Altered expression levels of ETS-transcription factors are often observed in many different tumors, including lymphomas. Here, we characterized two ETS inhibitors, YK-4-279 and its clinical derivative, TK-216, for their antilymphoma activity. Both compounds demonstrated an antitumor activity across several lymphoma cell lines, synergized with the BCL2 inhibitor venetoclax, and, in activated B-cell–like type diffuse large B-cell lymphomas, they interfered with SPIB and IRF4 transcriptional program, synergizing with lenalidomide. Thus, the ETS inhibitor YK-4-279 and its clinical derivative, TK-216, represent a new class of agents with *in vitro* and *in vivo* antitumor activity in lymphomas.

been studied in ES, nothing is known about their efficacy and mechanism of action in lymphoma. In this study, we investigated the activity and the molecular mechanisms of these compounds as potential novel antilymphoma agents as single agents and in combination.

Materials and Methods

Evaluation of *in vitro* antitumor activity

In vitro antiproliferative activity for YK-4-279 was evaluated as described previously (17). For TK-216, cell lines were seeded in 384-well plates at the density of 2,000 cells/well using the VIAFLO 96/384 hand-held electronic channel pipette (Integra Biosciences AG) and then treated with D300e Digital Dispenser (Tecan). MTT and IC_{50} calculation were done similarly to the YK-4-279 as described previously (17). Validations were performed by seeding and treating cells manually (18). Cell lines (Supplementary Table S1) were all validated for their identity by short-tandem repeat DNA fingerprinting at IDEXX BioResearch (19) or with the Promega GenePrint 10 System kit (20), and all the experiments were performed within 1 month from being thawed. Cells were periodically tested to confirm *Mycoplasma* negativity using the MycoAlert Mycoplasma Detection Kit (Lonza). *BCL2*, *MYC*, and *TP53* status were defined as described previously (21) and *MYD88* and *CARD11* mutational status was retrieved from Pasqualucci and colleagues (2). Evaluation of apoptosis, cell-cycle analysis, and combinations were performed as described previously (17). Combination Index (CI) values are referred as median CIs obtained exposing cell lines (72 hours) to eight increasing concentrations of two compounds alone or together. Concentrations that gave 10% or less of proliferation already with the single agent were discarded for further analyses. YK-4-279 was manufactured and separated into enantiomers with the purity determined by high-performance liquid chromatography, and the structure by nuclear magnetic resonance (AMRI); TK-216 was provided by Oncternal Therapeutics; lenalidomide and pomalidomide were purchased from Selleckchem.

In vivo experiments

NOD-Scid (NOD.CB17-*Prkdcscid*/NCrHsd) mice were subcutaneously inoculated, and tumor volumes were calculated and analyzed as described previously (18). Mouse maintenance and animal experiments were performed with study protocols approved by the local Swiss Cantonal Veterinary Authority (No. Ti-23-2015). YK-4-279 and TK-216 were dissolved in labrasol/tetraglycol/water at the proportion 72/8/20; lenalidomide was dissolved in PBS/10% DMSO. Differences in tumor volumes between treatment groups were calculated using the Mann–Whitney test (GraphPad Prism v. 7.0d, GraphPad Software). The *P* value for significance was <0.05.

IHC

Tumor tissues were fixed in 10% formalin solution, processed, and embedded in paraffin. IHC analysis was performed on tumors from the vehicle control or treatments groups. Tumor sections were stained for Ki67 (proliferation marker) or cleaved caspase-3 (apoptosis marker). IHC was performed on a Leica Bond automated immunostainer using anti-Ki67 antibody (catalog no. ab16667, Abcam) at 1:400, and anti–cleaved caspase-3 antibody (catalog no. 9661, Cell Signaling Technology) at 1:1,000. Heat induced antigen retrieval was performed using Leica Bond Epitope Retrieval Buffer 2 (EDTA solution, pH9.0) for 20 minutes. Nonspecific antibody binding was blocked using 5% milk in PBS-T. Antibodies were detected using Novocastra Bond Refine Polymer Detection and visualized with 3′3- diaminobenzidine (DAB; brown). A hematoxylin nuclear counterstain (blue) was applied.

Transcriptome profiling

Microarray-based gene expression profiling was done using the HumanHT-12 v4 Expression BeadChp (Illumina), as described previously (17). Data mining was done using gene set enrichment analysis (GSEA; ref. 22) and limma using Carmaweb (23), as previously described (17). RNA-Seq of YK-4-279 and TK-216 was done using the NEBNext Ultra Directional RNA Library Prep Kit for Illumina (New England BioLabs Inc.) and the NEBNext Multiplex Oligos for Illumina (New England BioLabs Inc.) for cDNA synthesis and addition of barcode sequences. The sequencing of the prepools was performed using the NextSeq 500 (Illumina) with the NextSeq 500/550 High Output Kit v2.5 (75 cycles; Illumina). Samples were processed starting from stranded, single-ended 75 bp-long sequencing reads. RNA of TK-216 only treated cells underwent RNA-Seq analysis, as described previously (24). cDNA was synthesized from total mRNA using Illumina TruSeq RNA Library Prep Kit v2 with poly-A selection. Unstranded, paired-end sequencing was conducted on barcoded libraries. Sequencing was performed on a HiSeq2500 to a depth of >80 M reads with read length at least 100 bp. Data mining of RNA-Seq data was performed as described previously (25). GSEA (22) was performed on preranked lists GSEA, as described previously (17). From all analyses, statistically significant gene sets ($P < 0.05$, FDR < 0.1) and transcripts (absolute log FC > 0.1, $P < 0.05$) were retained. Raw data are available at the National Center for Biotechnology Information (NCBI) Gene Expression Omnibus (GEO) (http://www.ncbi.nlm.nih.gov/geo) database (microarray, GSE114022; RNA-Seq, GSE114637).

Western blotting and immunoprecipitations

Protein extraction, separation, and immunoblotting were performed as described previously (26) with anti-SPIB rabbit monoclonal (D4V9S, Cell Signaling Technology), anti-SPI1 (9G7, Cell Signaling Technology), and anti-GAPDH mouse monoclonal (FF26A, CNIO). Immunoprecipitations were done from 10^7 of cells, lysed in cold nondenaturing lysis buffer with 0.025%

Downloaded from http://aacrjournals.org/clincancerres/article-pdf/25/16/5167/1933678/5167.pdf by guest on 25 January 2025

Triton-X and Halt protease inhibitor cocktail (Thermo Fisher Scientific), using a 1:100 dilution of the antibody of interest overnight. After incubation with Magna ChIP Protein A magnetic beads (16-661, Millipore), immunoblotting was performed on eluted samples with anti-DHX9 rabbit monoclonal (EPR13521, Abcam), or anti-DDX5 rabbit monoclonal (EPR7239, Abcam), or anti-SPIB mouse monoclonal (4G5B3, Santa Cruz Biotechnology), or anti-SPI1 (9G7, Cell Signaling Technology), all at 1:1,000 dilutions.

Results

ETS inhibitors have *in vitro* antitumor activity in lymphoma

We started evaluating the activity of the small molecule YK-4-279 on a panel of 44 lymphoma cell lines. The compound showed a dose-dependent antiproliferative activity in most of the cell lines (Table 1A; Supplementary Table S2). The activity was observed in cell lines derived from ABC-DLBCL (n. = 8, median IC_{50} = 405 nmol/L); GCB-DLBCL (n. = 17, 462 nmol/L), mantle cell lymphoma (MCL, n. = 10, 451 nmol/L), marginal zone lymphoma (MZL, n. = 3, 244 nmol/L), chronic lymphocytic leukemia (CLL, n. = 1, 994 nmol/L), peripheral T-cell lymphoma-not otherwise specified (PTCL-NOS, n. = 1, 1,029 nmol/L), and anaplastic large-cell lymphoma (ALCL, n. = 4, 368 nmol/L). Experiments performed on seven DLBCL cell lines showed that the antiproliferative activity of YK-4-279 was dose-dependent using only the active (S) and not the inactive (R) enantiomer (Supplementary Fig. S1). Only (S)- and not (R)-YK-4-279 was able to induce apoptosis (Supplementary Fig. S2) in both ABC- and GCB-DLBCL cell lines, consistent with an enantiospecific effect (27).

Once the clinical derivative of YK-4-279 became available (15), we assessed its antitumor activity on a now larger panel of lymphoma cell lines (n. = 55). Similar to YK-4-279, TK-216 showed potent dose-dependent antiproliferative activity in most of the cell lines (Table 1B; Supplementary Table S2), which comprised ABC-DLBCL (n. = 8, median IC_{50} = 375 nmol/L), GCB-DLBCL (n. = 18, 374 nmol/L), MCL (n. = 10, 339 nmol/L), MZL (n. = 6, 292 nmol/L), CLL (n. = 2, 1.1 μmol/L), primary mediastinal large B-cell lymphoma (n = 1, 547 nmol/L), cutaneous T-cell lymphoma (n = 3, 645 nmol/L), PTCL-NOS (n. = 1, 436 nmol/L), and ALCL (n. = 5, 193 nmol/L), and canine DLBCL (n = 1, 815 nmol/L).

YK-4-279 and TK-216 presented a similar pattern of antiproliferative activity across the 43 cell lines treated with both drugs [Pearson ρ = 0.67; 95% confidence interval (CI), 0.46–0.80; P < 0.0001; Supplementary Fig. S3] and their antitumor activity was mainly cytotoxic. Annexin V staining and cell-cycle analysis in two ABC- and two GCB-DLBCL cell lines showed a time-dependent apoptosis (Fig. 1A and B) preceded by G_2–M arrest in all four cell lines (Fig. 1C).

The sensitivity to YK-4-279 and TK-216 did not differ based on lymphoma subtypes, *TP53* status or, within DLBCL cell lines, on the presence of *MYC* translocation, *MYD88* and *CARD11* mutations, but a trend for lower sensitivity was observed in cell lines bearing *BCL2* chromosomal translocation after YK-4-279 and TK-216 treatment (Supplementary Table S2).

Both YK-4-279 and TK-216 have *in vivo* antitumor activity

The *in vitro* antitumor activity of YK-4-279 and TK-216 was confirmed using TMD8 cell lines as an ABC-DLBCL xenograft model (Fig. 2). Compared with the control group, mice treated with YK-4-279 (100 mg/kg, twice a day, orally) presented a reduction in tumor growth evident at day 8, 11 (P < 0.01) and 13 after the start of the treatment (P not available on day 13 because control group required euthanasia due to excessive tumor volume). Antitumor activity was greater with TK-216. Compared with the control group mice treated with TK-216 (100 mg/kg, twice a day, orally) clearly presented a reduction in tumor growth at day 3 which become much apparent with time (day 5, 8, 11: P < 0.01). YK-4-279 treatment was well tolerated with no body weight loss. TK-216 was well tolerated with the exception of 2 of 9 mice with 10% of body weight loss after 5 days of treatment. The observed antitumor activity was confirmed at IHC with reduced $Ki67^+$ cells in TK-216 (39%, P = 0.03) and in YK-4-279 (50%, P = n.s.)-treated versus control mice (63%). A moderate increase in cleaved caspase-3–positive cells was also observed (18% vs. 15%, P = n.s., YK-4-279 vs. vehicle; 20% vs. 15%, P = n.s., TK-216 vs. vehicle; Supplementary Fig. S4).

Table 1. Antitumor activity of YK-4-279 (A) and TK-216 (B) in lymphoma cell lines

(A)

	Number of cell lines	Median IC_{50} (nmol/L)	95% CI
All cell lines	44	454	346–512
ABC-DLBCL	8	405	288–1,174
GCB-DLBCL	17	462	302–562
MCL	10	451	288–794
MZL	3	244	181–524
CLL	1	994	n.d.
ALCL	4	368	169–759
PTCL-NOS	1	1,029	n.d.

(B)

	Number of cell lines	Median IC_{50} (nmol/L)	95% CI
All cell lines	55	393	288–490
ABC-DLBCL	8	375	128–794
GCB-DLBCL	18	374	219–512
MCL	10	339	141–501
MZL	6	292	117–871
CLL	2	1,112	1,047–1,202
PMBCL	1	547	n.d.
Canine DLBCL	1	815	n.d.
CTCL	3	645	562–1,819
ALCL	5	193	120–537
PTCL-NOS	1	436	n.d.

NOTE: IC_{50}s obtained after 72-hour treatment of YK-4-279 or TK-216. A total of 44 cell lines were used for YK-4-279 and 55 cell lines for TK-216.
Abbreviations: n.d., not determined; PMBCL, primary mediastinal large B-cell lymphoma.

YK-4-279 and TK-216 show preferential synergism with lenalidomide and venetoclax

We then first evaluated the clinical derivative TK-216 in combination with a series of antilymphoma agents in DLBCL cell lines. The combination partners were, in alphabetical order, the BCL2 inhibitor venetoclax, the BET inhibitor birabresib (OTX015), the chemotherapy agents bendamustine and vincristine, the dual PI3K/mTOR inhibitor bimiralisib (PQR309), the PI3K-delta inhibitor idelalisib, the XPO1 inhibitor selinexor, and the thalidomide-derived immunomodulatory drug (IMID) lenalidomide (Fig. 3; Supplementary Table S3). The BTK-inhibitor ibrutinib and the proteasome inhibitor bortezomib were tested only in cell lines derived from ABC-DLBCL, the subtype in which the drugs have reported clinical

Downloaded from http://aacrjournals.org/clincancerres/article-pdf/25/16/5167/1933678/5167.pdf by guest on 25 January 2025

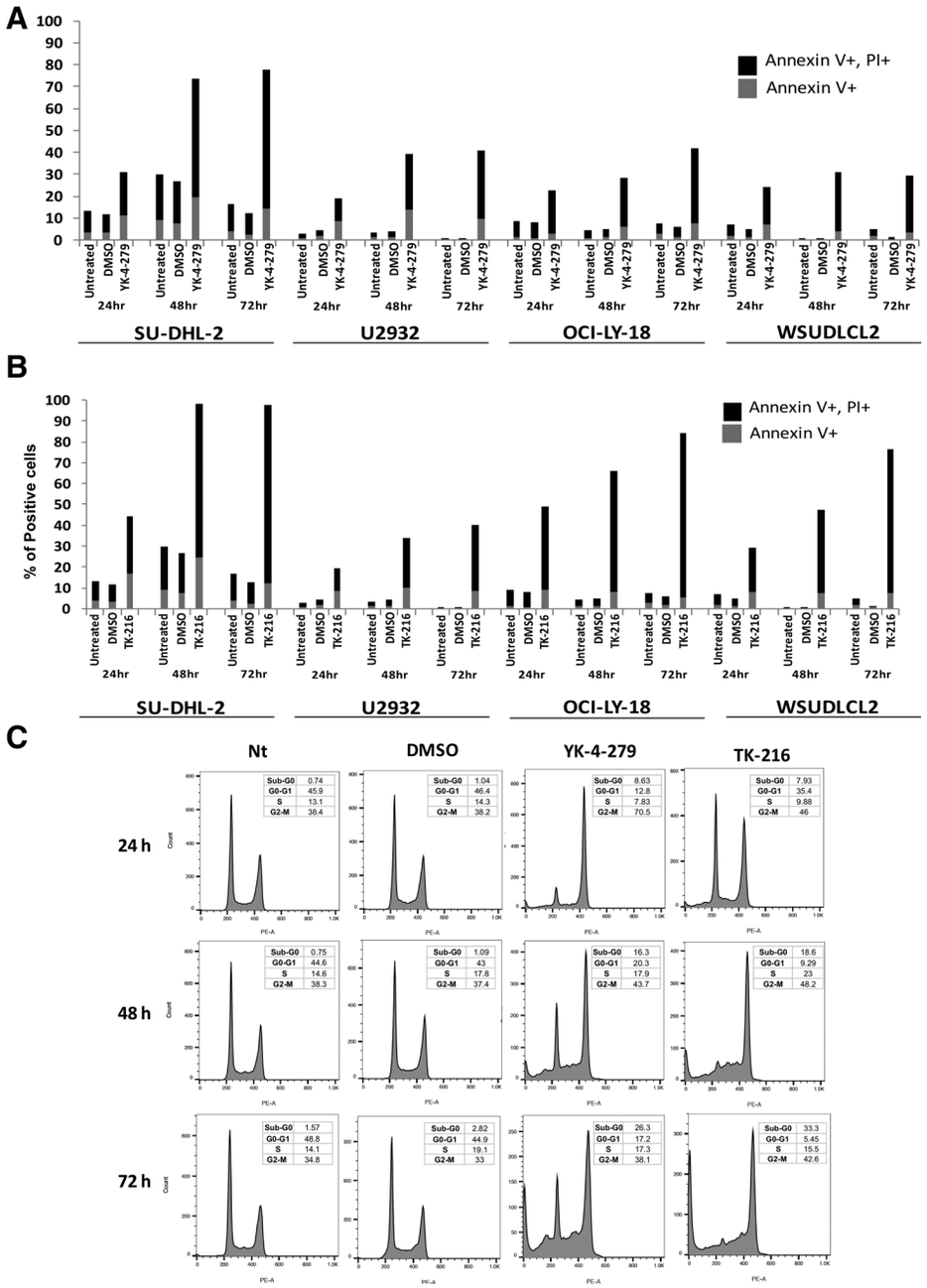

Figure 1.
Apoptosis in DLBCL cell lines exposed to YK-4-279 (**A**) or TK-216 (**B**) and cell-cycle distribution in U2932 (**C**). Four DLBCL cell lines (two ABC and two GCB) were either untreated (NT) or treated with YK-4-279 (**A**) or TK-216 (**B**; both at 500 nmol/L) accompanied by DMSO as solvent control for 24, 48, and 72 hours. The figure shows representative results from experiments performed in triplicate. At each time point, cells were subject to apoptosis (**A** and **B**) and cell cycle (**C**; U2932 is shown as representative).

activity. Synergism was noted when TK-216 was combined with venetoclax in 3 of 4 DLBCL. However, the most striking effect was observed when TK-216 was used together with lenalidomide (synergism in all four ABC-DLBCL). These results led us to also evaluate the combination in cell lines derived from MCL in which lenalidomide is also clinically active: synergy was observed in both MCL models (REC1 and Mino). We also treated two ABC-DLBCL cell lines with pomalidomide, a newer IMID, obtaining a synergistic effect in the pomalidomide less sensitive cell line and an additive effect in the more sensitive one. Similarly, synergy was also observed when YK-4-279 was combined with lenalidomide in 2 of 2 ABC-DLBCL cell lines and with the venetoclax combination in 2 of 4 DLBCL cell lines (Fig. 3; Supplementary Table S3).

The *in vitro* synergism with lenalidomide was validated with the clinical derivative TK-216 *in vivo* using the ABC-DLBCL cell line OCI-LY-10. Mice were treated with TK-216 (100 mg/kg, orally, twice a week), lenalidomide (20 mg/kg, i.p., five days a week) alone or in combination. The combination showed a higher antitumor activity compared with control group ($P < 0.01$, day 22) and to lenalidomide ($P < 0.01$, day 25) or TK-216 ($P < 0.05$, day 29) alone (Fig. 4A). Treatment with TK-216 alone, compared with the control group, significantly improved the survival of mice ($P < 0.05$) and this was further improved with combination

Downloaded from http://aacrjournals.org/clincancerres/article-pdf/25/16/5167/1933678/5167.pdf by guest on 25 January 2025

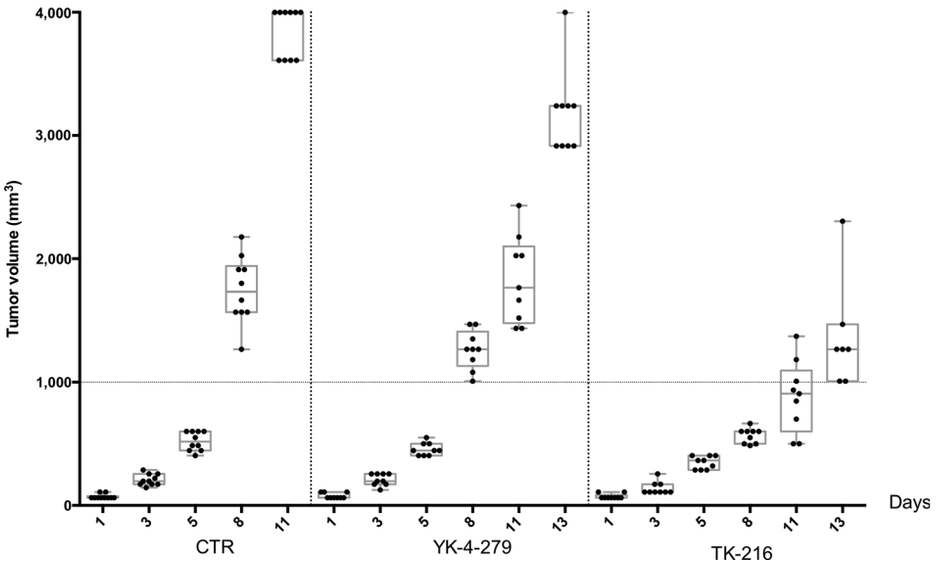

Figure 2.

Effects of YK-4-279 and TK-216 in the ABC-DLBCL xenograft model. NOD-Scid mice subcutaneously inoculated with TMD8 cells (15×10^6) were split in three groups, respectively, treated with TK-216 or YK-4-279 (100 mg/kg, twice a day, orally, $n = 9$) or control vehicle ($n = 10$). Compared with the control group, mice treated with YK-4-279 presented a statistically significant reduction in tumor growth at days 8 and 11 ($P < 0.01$) after the start of the treatment. Compared with the control group, mice treated with TK-216 presented a statistically significant reduction in tumor growth at days 5, 8, and 11 ($P < 0.01$). *P* values were not available on day 13 because the control group required euthanasia due to excessive tumor volume. In each box-plot, the line in the middle of the box represents the median and the box extends from minimum to maximum tumor volume.

lenalidomide treatment ($P < 0.01$; Fig. 4B). In this model, the schedule of TK-216 was modified from the previous *in vivo* experiment. Despite TK-216 was administrated twice a week instead of twice a day, antitumor activity compared with control group was preserved, and no body weight loss was observed in any treatment group.

We then investigate the possible mechanisms sustaining the two active combinations. In ABC-DLBCLlenalidomide has a direct antitumor activity targeting SPIB and IRF4 (28). Thus, we exposed the ABC-DLBCL cell line OCI-LY10 to TK-216 (500 nmol/L), lenalidomide (10 μmol/L) alone, and to the combination for 3, 6, and 24 hours. At the last time point, we observed a decrease in SPIB protein levels with both compounds as single agents, and a more pronounced effect with the combination (Supplementary Fig. S5A). The same was confirmed in the U2932, a second ABC-DLBCL cell line (Supplementary Fig. S5B). No effects were observed on IRF4 levels with combination treatment.

On the basis of the possible mechanisms leading to active venetoclax-containing combinations (29), we then exposed the ABC-DLBCL TMD8 to TK-216 and to the BCL2 inhibitor as single agents or in combination. The exposure to TK-216 was associated with decreased levels of the antiapoptotic proteins MCL1 and BCL2 (Supplementary Fig. S6).

YK-4-279 and TK-216 induce similar transcriptional changes and interfere with SPIB/IRF4 targets in ABC-DLBCL cell lines

To gain insight into the mechanism of action of YK-4-279, we had performed gene expression profiling (GEP) in ABC-DLBCL cell lines (U2932 and TMD8), treated with its active or inactive enantiomers at 500 nmol/L for 4 and 8 hours. At gene level, we observed 183 and 221 annotated genes, downregulated and upregulated, respectively, (Supplementary Table S4A). Transcripts upregulated in treated cells were enriched for genes involved in cell cycle, DNA repair, protein secretion, glycolysis, reactive oxygen species pathway, and IRF4 targets in multiple myeloma. Conversely, transcripts downregulated after exposure to (S)-YK-4-279 were enriched for genes involved in IFNα response and KRAS signaling (Supplementary Table S4B). Having observed the synergism between YK-4-279 and lenalidomide, which acts via modulation of the IRF4–SPIB axis (28), and the overlap of our GEP changes with IRF4 targets, we further investigated the effect of the small molecule on SPIB- and IRF4-regulated genes. Cell lines exposed to YK-4-279 showed upregulation of IRF4- and SPIB-repressed genes in ABC-DLBCL and downregulated genes also affected by lenalidomide (Supplementary Table S4C). Besides affecting the abovementioned pathways, YK-4-279 exposure also upregulated small nucleolar RNAs (snoRNA; Supplementary Table S4A).

Once TK-216 became the compound heading to clinical trials, we first evaluated the similarities of the compounds in multiple assays. Because YK-4-279 and TK-216 presented similar patterns of antitumor activity across all the cell lines and similar synergism with other compounds, we performed an RNA-Seq experiment to assess whether the two compounds had also a similar effect on lymphoma transcriptome. Four ABC-DLBCL lymphoma cell lines (U2932, TMD8, OCI-LY-10, and SU-DHL-2) were exposed to DMSO, YK-4-279, or TK-216 for 18 hours, based on a previous transcriptome study in ES (Supplementary Table S5; ref. 24). The induced transcriptome changes were highly correlated (Pearson ρ 0.67; 95% CI, 0.65–0.68; $P < 0.001$; Supplementary Fig. S7). Largely in accordance with what seen using the microarray platform in YK-4-279–treated cells, a genome-wide functional annotation of the affected transcripts (Supplementary Table S5A)

Downloaded from http://aacrjournals.org/clincancerres/article-pdf/25/16/5167/1933678/5167.pdf by guest on 25 January 2025

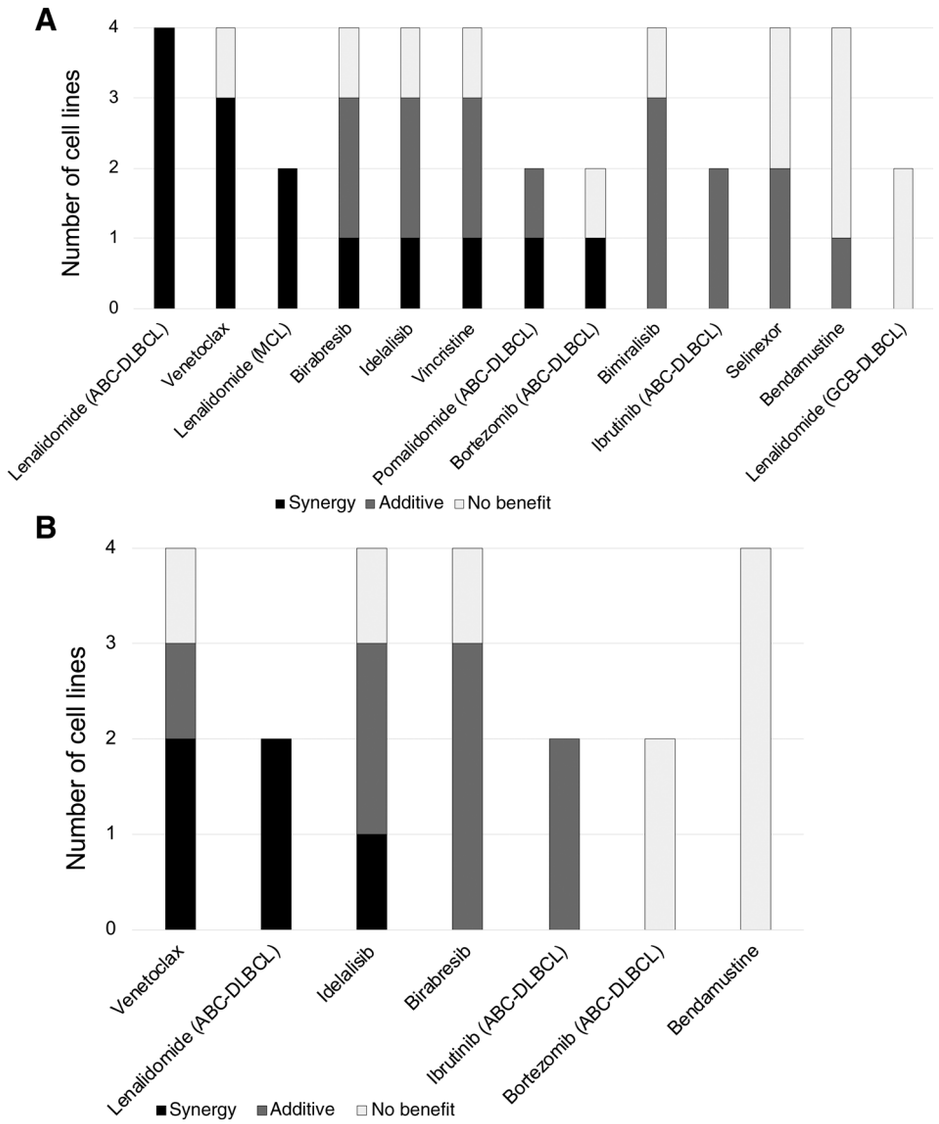

Figure 3.
TK-216 (**A**) and YK-4-279 (**B**) combinations in lymphoma cell lines. Drugs were tested in both GCB- and ABC-DLBCL if not otherwise stated. Synergism, additive effect, and no benefit were defined using the Chou–Talalay Combination Index (CI). Results for all the individual cell lines are shown in Supplementary Table S3. Synergism, CI < 0.9; additive effect, 0.9 < CI < 1.1; no benefit, CI >1.1.

showed that the two compounds shared an enrichment of the upregulated transcripts for genes involved in RNA splicing and processing, protein translation, ribosome biogenesis, P53 pathway, Myc targets, apoptosis, and DNA repair (Supplementary Table S5B). The downregulated transcripts were characterized by genes involved in DNA elongation and G_1–S–specific transcription, in line with the G_1–S decrease seen at cell-cycle analysis in cells exposed to TK-216 or YK-4-279. At gene level, we observed 436 and 816 genes downregulated after YK-4-279 and TK-216, respectively, and 252 and 624 genes upregulated.

Unexpectedly, we did not observe an enrichment of IRF4 or SPIB targets among genes affected by YK-4279 or TK-216 at 18 hours. Thus, we focused again on an earlier time point. The ABC-DLBCL cell line U2932 was exposed to TK-216 (500 nmol/L, 8 hours) and changes at transcriptome level were analyzed (Supplementary Table S6A). At gene level, we observed 202 and 79 downregulated and upregulated, respectively. Besides seeing changes similar to what observed at 18 hours (ribosome biogenesis, RNA splicing and processing, cell cycle), we did observe the enrichment for genes negatively regulated by IRF4 and SPIB (28, 30) in the TK-216–induced (Supplementary Table S6B, GSEA). On the contrary, genes positively regulated by IRF4 and SPIB were similarly decreased by TK-216 (Supplementary Table S6C). This difference between 8 and 18 hours suggests that the effect on SPIB/IRF4 targets is an early event in the mechanism of action of the small molecules in ABC-DLBCLs. Given the similarities of YK-4-279 and TK-216, we did further studies with TK-216 as this compound would enter clinical trials.

TK-216 targets SPIB in ABC-DLBCL

SPIB is an essential gene for ABC-DLBCL (5–7) and we have observed that TK-216 interferes with SPIB targets. YK-4-279 is known to reduce the binding between EWS-FLI1 and the RNA helicases DHX9 and DDX5 in ES models (9, 24). We explored, via coimmunoprecipitation experiments, whether a similar phenomenon might occur with TK-216 in ABC-DLBCL with SPIB in place of the fusion protein. SPIB showed binding to the two

Downloaded from http://aacrjournals.org/clincancerres/article-pdf/25/16/5167/1933678/5167.pdf by guest on 25 January 2025

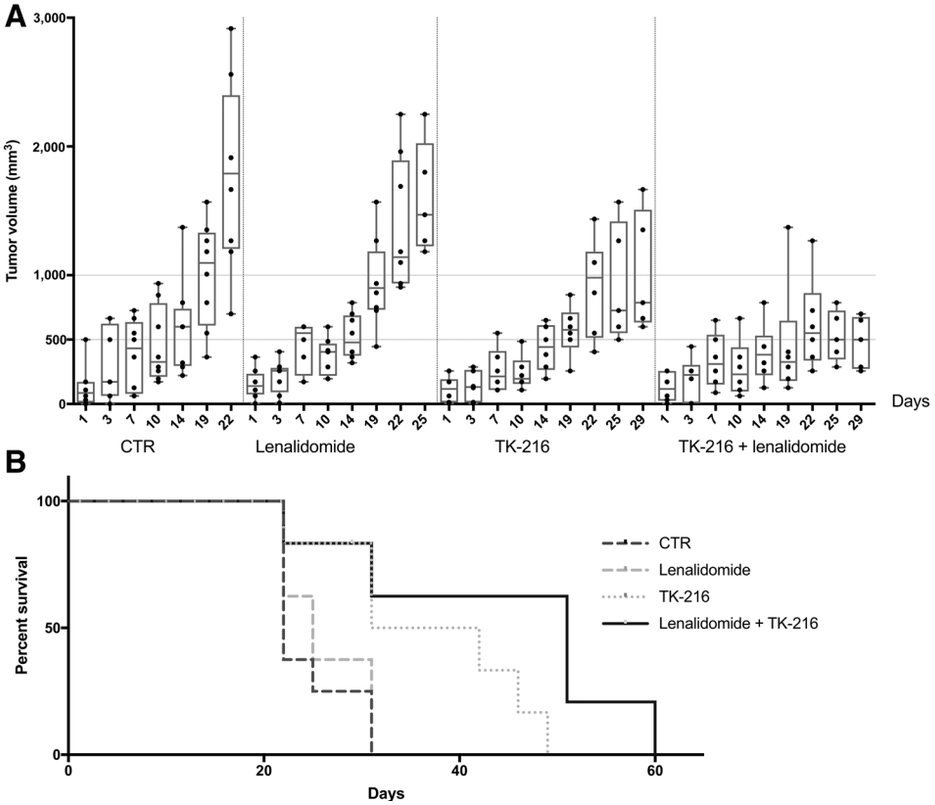

Figure 4.
In vivo synergy between TK-216 and lenalidomide. **A,** OCI-LY-10 cells were injected subcutaneously in NOD-SCID mice. Day 1 represents the start of treatment, when tumor reached 150 mm^3 approximately. Mice were divided in 4 groups: control vehicle ($n = 8$), lenalidomide (20 mg/kg, i.p., 5 days a week, $n = 8$), TK-216 (100 mg/kg, orally, two days a week, $n = 6$), and lenalidomide+TK-216 combination ($n = 6$). The combination showed a higher antitumor activity compared with the control group ($P < 0.01$, day 22) and to lenalidomide ($P < 0.01$, day 25) or TK-216 ($P < 0.05$, day 29) alone. In each box plot, the line in the middle of the box represents the median and the box extends from minimum to maximum tumor volume. **B,** Kaplan–Meier plot. Day 0 represents the start of the treatments. Treatment with TK-216 alone improved the survival of mice compared with the control group ($P < 0.05$), and the differences were bigger with the lenalidomide combination ($P < 0.01$).

RNA helicases in two ABC-DLBCL cell lines, and treatment of ABC-DLBCL cells with TK-216 for 4 hours decreased the binding of the ETS transcription factor to DHX9 and to a lesser extent DDX5 (Fig. 5A; Supplementary Fig. S8).

TK-216 targets SPI1 in GCB-DLBCL

The observed activity on SPIB could not justify the widespread antitumor activity across different lymphoma subtypes. A recent work has shown that SPI1 (PU.1) is an ETS factor

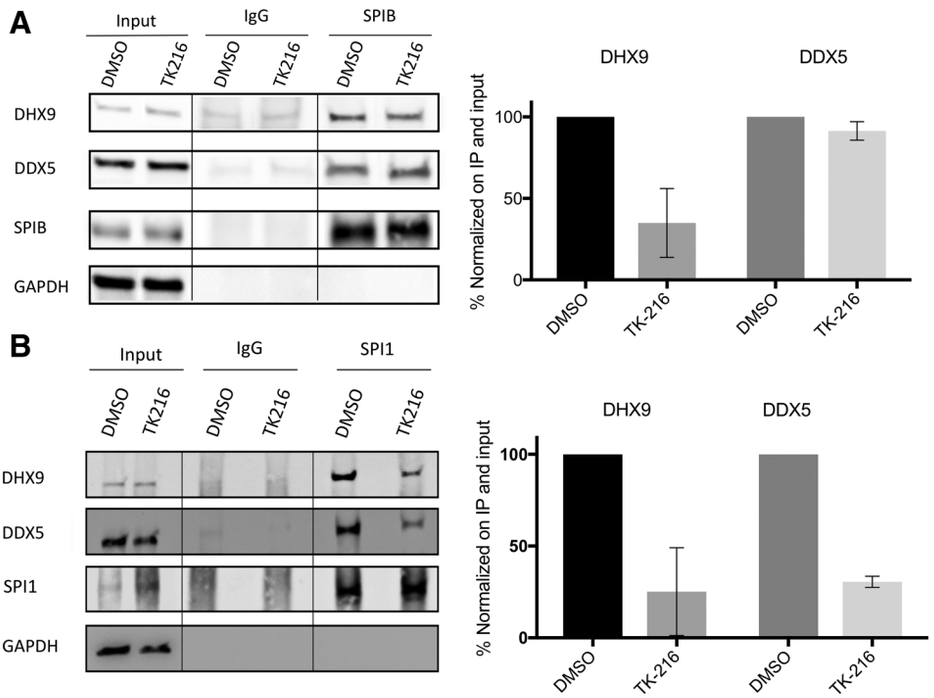

Figure 5.
TK-216 coimmunoprecipitations ABC- and GCB-DLBCL cell lines. Representative coimmunoprecipitation experiments with the respective densitometry after immunoprecipitation of SPIB in TMD8 (**A**) and SPI1 in DOHH2 (**B**). Coimmunoprecipitations were performed after 4 hours of treatment with TK-216 (1 μmol/L). IgG was used as immunoprecipitation-negative control. GAPDH was used as loading control.

Downloaded from http://aacrjournals.org/clincancerres/article-pdf/25/16/5167/1933678/5167.pdf by guest on 25 January 2025

essential for the survival of GCB-DLBCL (7). Hence, we performed coimmunoprecipitation experiments in the GCB-DLBCL cell line DOHH2. Similar to what seen for SPIB in ABC-DLBCL, also SPI1 was shown to bind to DHX9 and DDX5. Exposure to TK-216 reduced the binding between the ETS factor and the helicases (Fig. 5B).

Discussion

Our data show that the small molecule YK-4-279 and its clinical derivative TK-216 have significant *in vitro* and *in vivo* antitumor activity in lymphomas. The two molecules showed a similar pattern of antitumor activity across the cell lines and a similar effect at transcriptomic level. Both molecules were active in the vast majority of the lymphoma cell lines, irrespective of histology or main genetic and biologic features. Importantly, compared with other novel anticancer compounds (17, 18, 31), they also have cytotoxic activity. YK-4-279 was discovered following a screening program designed to identify peptides able to block the interaction between DHX9 and EWS-FLI1 created by the t(11;22)(q24;q12) chromosomal translocation in ES (9, 32). YK-4-279 shows antitumor activity in tumors expressing ETS factors, such as ES (9, 24, 27, 32–34) but also in ETS-driven prostate cancers (11–14). In ES, YK-4-279 inhibits the binding of the EWS-FLI1 fusion protein to RNA helicases, namely DHX9 and DDX5 (9, 24). We show that, in ABC-DLBCL, TK-216 interferes with the ETS factor SPIB decreasing its protein–protein interaction with the two helicases and also its expression levels. SPIB is an important transcription factor in B-cell development (35, 36), recurrently gained in ABC-DLBCL, and necessary for the survival of cell lines derived from this lymphoma (5–7). In ABC-DLBCL, SPIB interacts with IRF4, coregulating many shared target genes (28, 30), and its genetic silencing increased the sensitivity of the lymphoma cells to lenalidomide (28). In agreement, transcriptome analyses show that TK-216 had a strong effect on genes that are SPIB and IRF4 direct targets. Furthermore, YK-4-279 and TK-216 were synergistic with lenalidomide in both ABC-DLBCL and MCL cell lines, two tumors in which lenalidomide has a direct antitumor effect interfering with SPIB and IRF4 (28, 37, 38). The addition of lenalidomide caused stronger SPIB downregulation than either of the single agents alone. The synergism between TK-216 and lenalidomide in ABC-DLBCL was also confirmed *in vivo*.

Another synergistic interaction was found between the two ETS inhibitors with the BCL2 inhibitor venetoclax. Cotreatment with TK-216 led to reduced levels of BCL2 and MCL1. Consistently, YK-4-279 has a similar effect in ES (39) Our data indicate that the combination is worth of further investigations for its possible clinical implication.

The activity via SPIB and IRF4 cannot fully explain the observed antitumor activity of YK-4-279 and TK-216 in all the different lymphoma subtypes. *SPI1* (PU.1), a member of the same ETS subfamily of SPIB, has been recently demonstrated to be a gene essential for the survival of GCB-DLBCL, in contrast with *SPIB*, essential for the ABC-DLBCL (7). Similar to SPIB, we demonstrated in GCB-DLBCL cells, SPI1 binds to DDX5 and DHX9, and that TK-216 disrupts the binding. These data indicate that YK-4-279 and TK-216 can exert their antitumor activity in different lymphoma subtypes interfering with the function of different ETS factors. This is similar to different ETS-driven subgroups of prostate cancer (11–14).

Further work is certainly still needed to identify the individual ETS factors and to fully elucidate the compounds' mechanism of action. ETS transcription factors contribute to RNA processing (40), as demonstrated for the EWS-FLI1 fusion protein (24) and, here, by the interaction between SPIB or SPI1 with the RNA helicases DDX5 and DHX9, and the changes of genes coding for proteins involved in RNA splicing and processing after drugs expsoure. Blocking the binding of additional proteins or coregulatory transcription factors to ETS transcription factors (1) might contribute to the mechanism of action of the two small molecules. The observed arrest in G_2–M and the gene expression changes indicate that the small molecules might also interfere with tubulin polymerization, as suggested in solid tumor models (39, 41, 42), possibly exerting antitumor activity also in an ETS-independent manner.

Finally, we also observed an upregulation of snoRNAs, a type of small noncoding RNAs implicated in a broad range of biological functions including the regulation of ribosomes and of fundamental cancer proteins by directly binding to them or affecting their posttranslational modifications or their RNA molecules (43–48). The role of snoRNAs in lymphoid neoplasms has not yet been fully explored (49, 50) and they appear largely reduced in tumors compared with normal tissue counterparts (49). In accordance with these preliminary findings, their upregulation after treatment could contribute to the antitumor activity of the two small molecules in lymphoma and be strictly linked with the observed changes of genes involved in ribosome processing and RNA splicing genes. Indeed, snoRNAs processing might be affected because of the interference of YK-4-279 and TK-216 with RNA helicases and the splicing process. The majority of snoRNAs are processed from introns of coding or noncoding transcripts, while others have their own promoters. Comparing our list of snoRNAs upregulated by YK-4-279 treatment in ABC-DLBCL and ChIP-seq data obtained in ABC-DLBCL (28, 30), we identified at least ten snoRNAs as direct targets of SPIB. This observation, in agreement with the notion that also ETS2 directly regulates snoRNAs (45), indicates that the upregulation of snoRNAs might also be directly linked to the interference of YK-4-279 and TK-216 with the activity of ETS factors.

In conclusion, the ETS inhibitors YK-4-279 and its clinical derivative TK-216 represent a new class of agents with *in vitro* and *in vivo* antitumor activity in lymphomas that, in DLBCL, act by targeting subtype-specific essential transcription factors. Their detailed mechanism of action needs to be further defined in individual lymphoma types. A clinical trial is currently being designed with TK-216 for patients with relapsed and refractory lymphoma. The concept that ETS proteins can be viable drug targets is paradigm shifting in oncology such that these proteins, once deemed "undruggable" are now important to consider for future therapeutics.

Disclosure of Potential Conflicts of Interest

K. Jessen has ownership interests (including patents) in Oncternal. E. Zucca is a consultant/advisory board member for Celgene, Roche, Mei Pharma, AstraZeneca, and Celltrion Healthcare; has provided expert testimony for Gilead, Bristol-Myers Squibb, and MSD; and has received travel grants from AbbVie and Gilead. A. Stathis reports receiving commercial research grants from Bayer, ImmunoGen, Merck, Pfizer, Novartis, and Roche, and has received travel grants from AbbVie and Pharmamar. B. Lannutti has ownership interests (including patents) in Oncternal. J.A. Toretsky has ownership interests in, is a consultant/advisory board member for, and reports receiving commercial

Downloaded from http://aacrjournals.org/clincancerres/article-pdf/25/16/5167/1933678/5167.pdf by guest on 25 January 2025

research grants from Oncternal Therapeutics. F. Bertoni is a consultant for Helsinn and Menarini; reports receiving commercial research grants from Acerta, Bayer AG, Cellestia, CTI Life Sciences, EMD Serono, Helsinn, Immuno-Gen, Menarini Richerche, NEOMED Therapeutic Development, Oncology Therapeutic Development, and PIQUR Therapeutics AG, and expert statements provided to HTG. No potential conflicts of interest were disclosed by the other authors.

Authors' Contributions

Conception and design: E.Y.L. Chung, B. Lannutti, J.A. Toretsky, F. Bertoni
Development of methodology: F. Spriano, E.Y.L. Chung, E. Gaudio, L. Cascione, K. Jessen, B. Lannutti, F. Bertoni
Acquisition of data (provided animals, acquired and managed patients, provided facilities, etc.): F. Spriano, E.Y.L. Chung, E. Gaudio, C. Tarantelli, K. Jessen, L. Carrassa, G. Graham, B.H. Ye, B. Lannutti, F. Bertoni
Analysis and interpretation of data (e.g., statistical analysis, biostatistics, computational analysis): F. Spriano, E.Y.L. Chung, L. Cascione, K. Jessen, G. Graham, A. Cavalli, I. Kwee, B. Lannutti, F. Bertoni
Writing, review, and/or revision of the manuscript: F. Spriano, E.Y.L. Chung, E. Gaudio, C. Tarantelli, S. Napoli, K. Jessen, L. Carrassa, V. Priebe, S.P. Selvanathan, A. Cavalli, E. Zucca, A. Stathis, B. Lannutti, J.A. Toretsky, F. Bertoni
Administrative, technical, or material support (i.e., reporting or organizing data, constructing databases): F. Spriano, L. Cascione, F. Bertoni
Study supervision: E.Y.L. Chung, K. Jessen, F. Bertoni
Others (performed experiments): S. Napoli, L. Carrassa, V. Priebe, G. Sartori, A. Rinaldi, M. Testoni, D. Genini

Acknowledgments

This work was supported by funding from Oncosuisse KLS-3580-02-2015 (to F. Bertoni), Leukemia & Lymphoma Society #6521-17 (to F. Bertoni and J.A. Toretsky), Gelu Foundation (to J.A. Toretsky), and the Italian Association for Cancer Research (AIRC), Milan, Italy (MFAG 14456 to L. Carrassa).

The costs of publication of this article were defrayed in part by the payment of page charges. This article must therefore be hereby marked *advertisement* in accordance with 18 U.S.C. Section 1734 solely to indicate this fact.

Received August 20, 2018; revised February 18, 2019; accepted May 31, 2019; published first June 10, 2019.

Downloaded from http://aacrjournals.org/clincancerres/article-pdf/25/16/5167/1933678/5167.pdf by guest on 25 January 2025

References

1. Sharrocks AD. The ETS-domain transcription factor family. Nat Rev Mol Cell Biol 2001;2:827–37.
2. Pasqualucci L, Trifonov V, Fabbri G, Ma J, Rossi D, Chiarenza A, et al. Analysis of the coding genome of diffuse large B-cell lymphoma. Nat Genet 2011;43:830–7.
3. Bonetti P, Testoni M, Scandurra M, Ponzoni M, Piva R, Mensah AA, et al. Deregulation of ETS1 and FLI1 contributes to the pathogenesis of diffuse large B-cell lymphoma. Blood 2013;122:2233–41.
4. Lenz G, Nagel I, Siebert R, Roschke AV, Sanger W, Wright GW, et al. Aberrant immunoglobulin class switch recombination and switch translocations in activated B cell-like diffuse large B cell lymphoma. J Exp Med 2007;204: 633–43.
5. Lenz G, Wright GW, Emre NC, Kohlhammer H, Dave SS, Davis RE, et al. Molecular subtypes of diffuse large B-cell lymphoma arise by distinct genetic pathways. Proc Natl Acad Sci U S A 2008;105:13520–5.
6. Reddy A, Zhang J, Davis NS, Moffitt AB, Love CL, Waldrop A, et al. Genetic and functional drivers of diffuse large B cell lymphoma. Cell 2017;171: 481–94.
7. Phelan JD, Young RM, Webster DE, Roulland S, Wright GW, Kasbekar M, et al. A multiprotein supercomplex controlling oncogenic signalling in lymphoma. Nature 2018;560:387–91.
8. Heerma van Voss MR, van Diest PJ, Raman V. Targeting RNA helicases in cancer: The translation trap. Biochim Biophys Acta 2017;1868:510–20.
9. Erkizan HV, Kong Y, Merchant M, Schlottmann S, Barber-Rotenberg JS, Yuan L, et al. A small molecule blocking oncogenic protein EWS-FLI1 interaction with RNA helicase A inhibits growth of Ewing's sarcoma. Nat Med 2009;15:750–6.
10. Toretsky JA, Erkizan V, Levenson A, Abaan OD, Parvin JD, Cripe TP, et al. Oncoprotein EWS-FLI1 activity is enhanced by RNA helicase A. Cancer Res 2006;66:5574–81.
11. Rahim S, Beauchamp EM, Kong Y, Brown ML, Toretsky JA, Uren A. YK-4-279 inhibits ERG and ETV1 mediated prostate cancer cell invasion. PLoS One 2011;6:e19343.
12. Rahim S, Minas T, Hong SH, Justvig S, Celik H, Kont YS, et al. A small molecule inhibitor of ETV1, YK-4-279, prevents prostate cancer growth and metastasis in a mouse xenograft model. PLoS One 2014;9:e114260.
13. Winters B, Brown L, Coleman I, Nguyen H, Minas TZ, Kollath L, et al. Inhibition of ERG activity in patient-derived prostate cancer xenografts by YK-4-279. Anticancer Res 2017;37:3385–96.
14. Yu L, Wu X, Chen M, Huang H, He Y, Wang H, et al. The effects and mechanism of YK-4-279 in combination with docetaxel on prostate cancer. Int J Med Sci 2017;14:356–66.
15. Selvanathan SP, Moseley E, Graham GT, Jessen K, Lannutti B, Üren A, et al. Abstract 694: TK-216: a novel, first-in-class, small molecule inhibitor of EWS-FLI1 in early clinical development, for the treatment of Ewing Sarcoma. In: Proceedings of the Annual Meeting of the American Association for Cancer Research; 2017 Apr 1-5; Washington, DC. Philadelphia (PA): AACR; 2017. p77:Abstract nr 694.
16. Federman N, Meyers PA, Daw NC, Toretsky J, Breitmeyer JB, Singh AS, et al. A phase I, first-in-human, dose escalation study of intravenous TK216 in patients with relapsed or refractory Ewing sarcoma. J Clin Oncol 35:15s, 2017(suppl; abstr TPS11626).
17. Tarantelli C, Gaudio E, Arribas AJ, Kwee I, Hillmann P, Rinaldi A, et al. PQR309 is a novel dual PI3K/mTOR inhibitor with preclinical antitumor activity in lymphomas as a single agent and in combination therapy. Clin Cancer Res 2018;24:120–9.
18. Boi M, Gaudio E, Bonetti P, Kwee I, Bernasconi E, Tarantelli C, et al. The BET bromodomain inhibitor OTX015 affects pathogenetic pathways in pre-clinical B-cell tumor models and synergizes with targeted drugs. Clin Cancer Res 2015;21:1628–38.
19. Mensah AA, Cascione L, Gaudio E, Tarantelli C, Bomben R, Bernasconi E, et al. Bromodomain and extra-terminal domain inhibition modulates the expression of pathologically relevant microRNAs in diffuse large B-cell lymphoma. Haematologica 2018;103:2049–58.
20. Tarantelli C, Bernasconi E, Gaudio E, Cascione L, Restelli V, Arribas AJ, et al. BET bromodomain inhibitor birabresib in mantle cell lymphoma: in vivo activity and identification of novel combinations to overcome adaptive resistance. ESMO Open 2018;3:e000387.
21. Hicks SW, Tarantelli C, Wilhem A, Gaudio E, Li M, Arribas AJ, et al. The novel CD19-targeting antibody-drug conjugate huB4-DGN462 shows improved anti-tumor activity than SAR3419 in CD19-positive lymphoma and leukemia models. Haematologica 2019 Feb 7 [Epub ahead of print].
22. Subramanian A, Tamayo P, Mootha VK, Mukherjee S, Ebert BL, Gillette MA, et al. Gene set enrichment analysis: a knowledge-based approach for interpreting genome-wide expression profiles. Proc Natl Acad Sci U S A 2005;102:15545–50.
23. Rainer J, Sanchez-Cabo F, Stocker G, Sturn A, Trajanoski Z. CARMAweb: comprehensive R- and bioconductor-based web service for microarray data analysis. Nucleic Acids Res 2006;34:W498–503.
24. Selvanathan SP, Graham GT, Erkizan HV, Dirksen U, Natarajan TG, Dakic A, et al. Oncogenic fusion protein EWS-FLI1 is a network hub that regulates alternative splicing. Proc Natl Acad Sci U S A 2015;112:E1307–16.
25. Cascione L, Rinaldi A, Bruscaggin A, Tarantelli C, Arribas AJ, Kwee I, et al. Novel insights into the genetics and epigenetics of MALT lymphoma unveiled by next generation sequencing analyses. Haematologica 2019 Apr 24 [Epub ahead of print].
26. Boi M, Rinaldi A, Kwee I, Bonetti P, Todaro M, Tabbo F, et al. PRDM1/BLIMP1 is commonly inactivated in anaplastic large T-cell lymphoma. Blood 2013;122:2683–93.
27. Barber-Rotenberg JS, Selvanathan SP, Kong Y, Erkizan HV, Snyder TM, Hong SP, et al. Single enantiomer of YK-4-279 demonstrates specificity in targeting the oncogene EWS-FLI1. Oncotarget 2012;3:172–82.

28. Yang Y, Shaffer AL 3rd, Emre NC, Ceribelli M, Zhang M, Wright G, et al. Exploiting synthetic lethality for the therapy of ABC diffuse large B cell lymphoma. Cancer Cell 2012;21:723–37.
29. Bose P, Gandhi V, Konopleva M. Pathways and mechanisms of venetoclax resistance. Leuk Lymphoma 2017;58:1–17.
30. Care MA, Cocco M, Laye JP, Barnes N, Huang Y, Wang M, et al. SPIB and BATF provide alternate determinants of IRF4 occupancy in diffuse large B-cell lymphoma linked to disease heterogeneity. Nucleic Acids Res 2014; 42:7591–610.
31. Meadows SA, Vega F, Kashishian A, Johnson D, Diehl V, Miller LL, et al. PI3Kdelta inhibitor, GS-1101 (CAL-101), attenuates pathway signaling, induces apoptosis, and overcomes signals from the microenvironment in cellular models of Hodgkin lymphoma. Blood 2012;119:1897–900.
32. Tosso PN, Kong Y, Scher L, Cummins R, Schneider J, Rahim S, et al. Synthesis and structure-activity relationship studies of small molecule disruptors of EWS-FLI1 interactions in Ewing's sarcoma. J Med Chem 2014;57:10290–303.
33. Hong SH, Youbi SE, Hong SP, Kallakury B, Monroe P, Erkizan HV, et al. Pharmacokinetic modeling optimizes inhibition of the 'undruggable' EWS-FLI1 transcription factor in Ewing sarcoma. Oncotarget 2014;5: 338–50.
34. Lamhamedi-Cherradi S-E, Menegaz BA, Ramamoorthy V, Aiyer RA, Maywald RL, Buford AS, et al. An oral formulation of YK-4-279: preclinical efficacy and acquired resistance patterns in Ewing sarcoma. Mol Cancer Ther 2015;14:1591–604.
35. Su GH, Chen HM, Muthusamy N, Garrett-Sinha LA, Baunoch D, Tenen DG, et al. Defective B cell receptor-mediated responses in mice lacking the Ets protein, Spi-B. EMBO J 1997;16:7118–29.
36. Schmidlin H, Diehl SA, Nagasawa M, Scheeren FA, Schotte R, Uittenbogaart CH, et al. Spi-B inhibits human plasma cell differentiation by repressing BLIMP1 and XBP-1 expression. Blood 2008;112:1804–12.
37. Solomon LA, Batista CR, DeKoter RP. Lenalidomide modulates gene expression in human ABC-DLBCL cells by regulating IKAROS interaction with an intronic control region of SPIB. Exp Hematol 2017;56:46–57.
38. Moros A, Rodriguez V, Saborit-Villarroya I, Montraveta A, Balsas P, Sandy P, et al. Synergistic antitumor activity of lenalidomide with the BET bromodomain inhibitor CPI203 in bortezomib-resistant mantle cell lymphoma. Leukemia 2014;28:2049–59.
39. Zollner SK, Selvanathan SP, Graham GT, Commins RMT, Hong SH, Moseley E, et al. Inhibition of the oncogenic fusion protein EWS-FLI1 causes G2-M cell cycle arrest and enhanced vincristine sensitivity in Ewing's sarcoma. Sci Signal 2017;10:pii: eaam8429.
40. Hallier M, Tavitian A, Moreau-Gachelin F. The transcription factor Spi-1/PU.1 binds RNA and interferes with the RNA-binding protein p54. J Biol Chem 1996;271:11177–81.
41. Seashore-Ludlow B, Rees MG, Cheah JH, Cokol M, Price EV, Coletti ME, et al. Harnessing connectivity in a large-scale small-molecule sensitivity dataset. Cancer Discov 2015;5:1210–23.
42. Kollareddy M, Sherrard A, Park JH, Szemes M, Gallacher K, Melegh Z, et al. The small molecule inhibitor YK-4-279 disrupts mitotic progression of neuroblastoma cells, overcomes drug resistance and synergizes with inhibitors of mitosis. Cancer Lett 2017;403:74–85.
43. Siprashvili Z, Webster DE, Johnston D, Shenoy RM, Ungewickell AJ, Bhaduri A, et al. The noncoding RNAs SNORD50A and SNORD50B bind K-Ras and are recurrently deleted in human cancer. Nat Genet 2016;48: 53–8.
44. Gong J, Li Y, Liu CJ, Xiang Y, Li C, Ye Y, et al. A pan-cancer analysis of the expression and clinical relevance of small nucleolar RNAs in human cancer. Cell Rep 2017;21:1968–81.
45. Pourebrahim R, Zhang Y, Liu B, Gao R, Xiong S, Lin PP, et al. Integrative genome analysis of somatic p53 mutant osteosarcomas identifies Ets2-dependent regulation of small nucleolar RNAs by mutant p53 protein. Genes Dev 2017;31:1847–57.
46. Hall KB. RNA and proteins: mutual respect. F1000Res 2017;6:345.
47. McMahon M, Contreras A, Ruggero D. Small RNAs with big implications: new insights into H/ACA snoRNA function and their role in human disease. Wiley Interdiscip Rev RNA 2015;6:173–89.
48. Dupuis-Sandoval F, Poirier M, Scott MS. The emerging landscape of small nucleolar RNAs in cell biology. Wiley Interdiscip Rev RNA 2015;6:381–97.
49. Valleron W, Ysebaert L, Berquet L, Fataccioli V, Quelen C, Martin A, et al. Small nucleolar RNA expression profiling identifies potential prognostic markers in peripheral T-cell lymphoma. Blood 2012;120:3997–4005.
50. Jima DD, Zhang J, Jacobs C, Richards KL, Dunphy CH, Choi WW, et al. Deep sequencing of the small RNA transcriptome of normal and malignant human B cells identifies hundreds of novel microRNAs. Blood 2010;116: e118–27.

Downloaded from http://aacrjournals.org/clincancerres/article-pdf/25/16/5167/1933678/5167.pdf by guest on 25 January 2025